ELSEVIER

Atmospheric Research 79 (2006) 89–107

ATMOSPHERIC RESEARCH

www.elsevier.com/locate/atmos

A 3-year study of cloud-to-ground lightning flash characteristics of Mesoscale convective systems over the Western Mediterranean Sea

Juan Francisco Correoso, Emiliano Hernández, Ricardo García-Herrera*, David Barriopedro, Daniel Paredes

Dept. Física de la Tierra II, Facultad de Ciencias Físicas, Universidad Complutense de Madrid, Ciudad Universitaria S/N, 28040 Madrid, Spain

Received 17 December 2004; received in revised form 10 May 2005; accepted 10 May 2005

Abstract

In this paper cloud-to-ground (CG) lightning flashes of 33 Mesoscale Convective Systems (MCSs) over the Western Mediterranean area are analyzed. Mean values of 22% for the positive CG ratio, 1.1 (2.4) for positive (negative) CG multiplicity, 17 kA (22.6 kA) of peak current for the positive (negative) CG flashes and a mean flash rate of around 13 $\min^{-1}$ are obtained. The percentage of positive CGs and the multiplicity of negative CG are higher, while the mean peak currents are lower than in previous studies on MCSs. A more detailed case analysis reveals that there are great differences among the CG characteristics of MCSs. The life cycle of CG lightning associated with MCSs is also analyzed. The growing stages of MCSs are characterised by high CG lightning activity. The positive CG flash rate generally reaches a maximum before the negative CG flash rate does. In both cases the peak is recorded before or when MCSs show the largest area. Maximum flash rate and densities coincide with the area where the MCS shows the minimum cloud-top temperatures and therefore shows highest vertical development.

Keywords: Mesoscale convective systems; Lightning; Meteosat; Western Mediterranean

* Corresponding author. Fax: +34 91 394 51 95.
E-mail address: rgarciah@fis.ucm.es (R. Garcia-Herrera).

0169-8095/$ - see front matter © 2005 Elsevier B.V. All rights reserved.
doi:10.1016/j.atmosres.2005.05.002

1. Introduction

One of the most important meteorological characteristics of the Western Mediterranean area are the heavy rainfall episodes that usually occur during summer and autumn, mainly from August to October. Most of these extreme precipitation events have a convective origin that can organize into a Mesoscale Convective System (MCS). The MCSs are a subset within the convective phenomena that evolve to long-lived storm systems and have dimensions much larger than individual storms.

The detection of MCSs is usually made from satellite imagery. Infrared (IR) radiance channel has been commonly chosen as the most accurate way to describe the evolution of convective systems because of its direct relationship with the cloud-top brightness temperature. Many tracking methods have been developed to follow the trajectories of convective systems in order to analyze their structural parameters as well as their spatial and temporal evolution (Machado et al., 1998; Morel and Senesi, 2002).

Convective activity in the Western Mediterranean area has been studied by some authors. Tuduri and Ramis (1997) studied the environments of significant convective events. Romero et al. (2000), Homar et al. (2002), among others, characterised MCSs using mesoscale numerical simulations. Moreover, Carretero and Riosalido (1996), Hernández et al. (1996) and García-Herrera et al. (2005a) used Meteosat satellite imagery to describe morphological and dynamical properties of the MCSs and the mesoscale convective complexes (MCCs) life cycle. Rainfall patterns associated with MCSs were also analyzed using radar, precipitation data and numerical simulations (Romero et al., 2001).

The temporal and spatial distribution of cloud-to-ground (CG) lightning activity in Iberia has been studied by several authors (Rivas et al., 2001, hereafter R01; Areitio et al., 2001, hereafter A01) and in the Western Mediterranean Sea for the 1992–1994 period (Rivas and De Pablo, 2002, hereafter RP02) but the studies of the characteristics of lightning activity associated with MCSs are still scarce in the region. Most of them have been made in the United States (e.g., Goodman and MacGorman, 1986; Morgenstern, 1991; Parker et al., 2001), while in the Western Mediterranean region only a few cases of CG lightning activity associated with storms in the Pyrenees area have been studied (Soula et al., 1998; Molinie et al., 1999). This paper analyses the CG lightning activity associated with the MCSs occurring during the 2000 to 2002 convective seasons (June to December). Meteosat-7 satellite imagery and CG lightning data are used. The paper is organized as follows. Section 2 gives a description of the data used. In Section 3 the general characteristics of the CG lightning activity of the MCSs in the Western Mediterranean Sea are presented. CG lightning life cycle is reported in Section 4 and, finally, the results are discussed in Section 5.

2. Data

Meteosat-7 infrared (IR) channel (10.5–12.5 μm) imagery (www.eumetsat.de), obtained from the Departamento de Física de la Tierra II (Universidad Complutense de Madrid), has been used as input of the Maximum Spatial Correlation Tracking Technique (MAS-

COTTE), developed by Carvalho and Jones (2001). The period studied includes from June to December during the years 2000, 2001 and 2002. The MASCOTTE is an objective and automated method to describe structural properties of the cloud shields derived from the IR imagery. It has been adapted to the Meteosat-7 imagery and to the Western Mediterranean area and has been used to identify and track MCSs occurring during the three studied seasons. MASCOTTE isolates, one by one, the systems fulfilling the identification criteria in the image t_i from the background and correlates the isolated system in the image t_i and all the possible candidates in the image t_{i+1}. The system in the image t_{i+1} representing the maximum correlation value over a minimum threshold, is considered the next spatial position of the isolated system in the image t_i. This technique is also used to compute mergings and splittings, which are important features in MCS life cycles. For each MCS identified by MASCOTTE, a set of structural properties is computed (position, mean velocity and direction of displacement, mean and minimum temperature, ratio between major and minor axis, among others). A more complete description of the MASCOTTE adaptation and performance in the Western Mediterranean can be seen in García-Herrera et al. (2005b).

The lightning detection system consists of a network of 13 sensors installed on the Iberian Peninsula and one on the Balearic Islands (Fig. 1) and is operated by the Spanish Institute of Meteorology (INM). The network detects and locates the ground strike location of CG lightning flashes, while intracloud discharges are filtered out by the system. They use Advanced Lightning Direction Finder (ALDF) model 141-T manufactured by Lightning Location and Protection Inc., which is currently known as Vaisala-Global Atmospheric Inc., Tucson, Arizona. Principles and characteristics of the lightning detection sensors have been discussed extensively by many authors (e.g., Krider et al.,

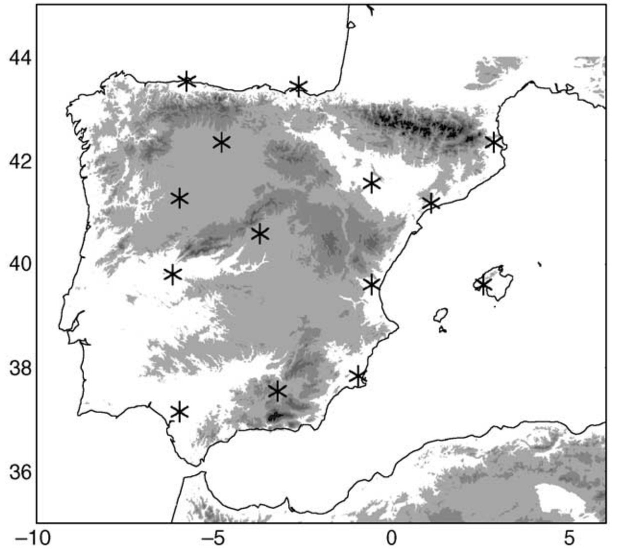

Fig. 1. Location of the CG lightning detection sensors installed on the Iberian Peninsula and the Balearic Islands. The shaded contours indicate the orography starting in 500 m (lighter) and in intervals of 500 m.

1976; Orville et al., 1983; Lopez and Holle, 1986). Each sensor contains a wideband system of orthogonal magnetic loop antennas and a flat plane electric antenna. The magnetic field of a lightning flash produces a signal in the circuit of each loop. Magnetic direction finding uses simple triangulation based on the intersection of azimuth bearings from two or more cross-looped antennas to locate a flash. A 180° ambiguity in direction is removed by an electric field antenna that senses the polarity of the charge lowered to the ground. The location accuracy of flashes with this system has been analyzed by Martín León (1995), who reported maximum error in the flash position lower than 8 km to 2 km, depending on the considered area. Detection efficiency has not yet been estimated. A direction finder automatically detects nearly 80–90% of all CG lightning occurring within a nominal detectable distance of 400 km. However, specially near the edges of the network the assumption of 80% uniform flash detection efficiency may not be realistic (a summary about the lightning network can be found in Cummins et al., 1998). Previous studies made in the area of the Iberian Peninsula (R01; Rivas and De Pablo, 2002) or in other places (Orville, 1994; Finke and Hauf, 1996) used an arbitrary detection efficiency of 70%. Nonetheless, this arbitrary assumption has not been proved in the Iberian Peninsula and the Balearic Islands and, in consequence, no attempt was made to correct for detection efficiency. The information obtained from the Spanish lightning detection network is the date and hour, position, amplitude of the first stroke and the number of strokes per flash (multiplicity).

3. General characteristics of CG lightning activity associated with MCSs

Each detected MCS has been isolated from its surroundings to study the general characteristics of the associated CG lightning activity. The number of CG lightning flashes during a 30-min interval has been obtained using the corresponding hour of each IR image as the temporal center of the interval. A test was made to establish the number of CGs associated with a MCS during the 30-min period, since the two datasets show different temporal resolutions (30 min for the satellite imagery and 1s for the CG flashes) and the position of an MCS can change during the 30-min interval between successive satellite images. The -52 °C brightness isotherm was chosen because it delimits the area of stronger rain and is well correlated with the cloud shield defined by other isotherms (Riosalido et al., 1998). Warmer temperatures may introduce errors due to the embedded of clouds not related with the MCS in the cloud shield associated with the system. An analysis of the CG flashes associated with an MCS in a lower temporal period (10 min) was made and it showed that most of them were located within the -52 °C or colder pixels. Finally, the CG lightning flashes included in a square with a margin of 0.2° latitude/longitude around the -52 °C brightness isotherm cloud shield position have been considered as associated with the MCSs. See Fig. 2 for an example. The margin has been chosen as 0.2° because the mean speed obtained in the study of García-Herrera et al. (2005b) for the same database of MCSs was 38 $km \cdot h^{-1}$ and during a 30-min period this implies a displacement of around 0.17°. Using the adapted MASCOTTE a total of 35 MCSs were detected over the Western Mediterranean (see García-Herrera et al., 2005b). Finally, 2 MCSs were discarded because they were too far from any lightning detection sensor during most of their life; thus a total of 33 MCSs were analyzed.

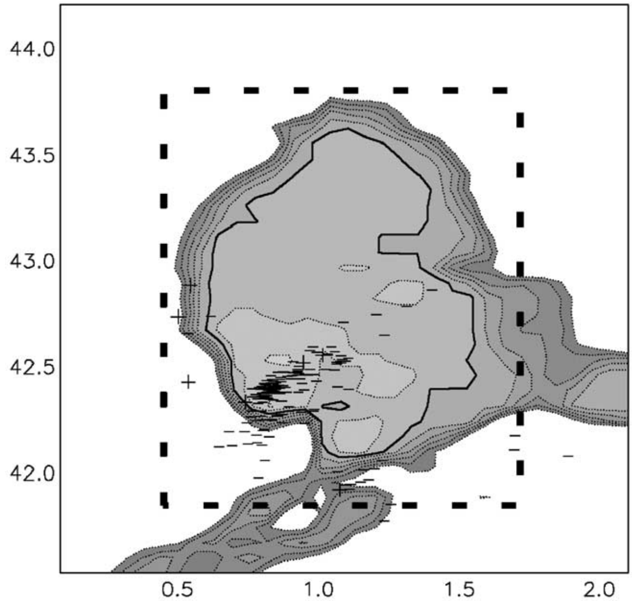

Fig. 2. MCS07 at 1330 UTC on 19 September 2000. The shaded contours indicate 4 °C brightness temperature intervals starting in −32 °C (darker). The solid line indicates the −52 °C cloud shield and the dashed square shows the area of the CG flashes considered as associated with the MCS during the 1315–1345 UTC interval. '+' and '−' indicate the position of the positive and negative CG flashes, respectively.

Table 1 shows some general characteristics of the CG lightning activity associated with the MCSs. Column 2 shows the date of the initiation of MCSs. Columns 3 and 4 show the +CG and −CG flashes recorded during the life cycle of MCSs considering the 30-min periods when an image was available. The percentage of all CG that were positive flashes is shown in column 5. Mean flash multiplicity (number of strokes per flash) of both polarities of CG flashes during the life cycle of MCSs is shown in columns 6 and 7. Columns 8 to 11 show the mean and median first stroke peak current CG flashes for each MCS (hereafter, mean and median peak current are referred to mean and median first stroke peak current). Columns 12 and 13 show the mean density of +CG and −CG flashes, respectively, in the area delimited by the −52 °C brightness isotherm. Maximum −52 °C cloud shield area is shown in column 14. In columns 15 and 16 the mean +CG and −CG flash rate during the life cycle of each MCS are displayed and, finally, column 17 shows the duration of the MCSs (divided in phases, see Section 4). The last row of Table 1 shows mean values and the standard deviation (computed by using the total number of flashes associated with the 33 cases) of the different parameters.

3.1. Polarity

In this section, the polarity of the first stroke has been used in the analysis. The average +CG flash ratio of the Western Mediterranean MCSs during our analysis period is around 22% (computed using all CG flashes associated with the MCSs), but with great variability

Table 1
General characteristics of MCSs (averaged over the entire life cycle)

MCS	Date yy/mm/dd	+CG	−CG	% +CG	Mult +CG	Mult −CG	Int +CG (kA) (mean)	Int −CG (kA) (mean)	Int +CG (kA) (median)	Int −CG (kA) (median)	Dens +CG (100 km^{-1} 30 min^{-1})	Dens −CG (100 km^{-1} 30 min^{-1})	Max. area	Flash rate (+CG/30 min)	Flash rate (−CG/30 min)	Duration (h)[a]
1	2000/06/26	1399	3037	31.5	1.1	1.7	28.3	16.7	14.7	12.6	0.16	0.35	97,336	78	169	1.5+4.5+3.5
2	2000/08/29	951	6371	13.0	1.1	1.9	32.6	20.1	21.9	16.3	0.18	1.23	49,902	50	335	0.5+2.5+4.5
3	2000/08/30	154	2368	6.1	1.1	2.4	34.3	26.7	22	19.2	0.09	1.41	19,944	11	169	3.0+1.0+2.0
4	2000/08/30	832	3639	18.6	1.1	2.1	21.7	16.1	10.1	12.8	0.37	1.63	55,776	92	404	1.0+2.5+3.5
5	2000/09/04	1049	3559	22.7	1.1	2.4	16.5	28.1	12.4	21.8	0.9	3.07	20,795	131	445	1.5+2.0+0.5
6	2000/09/19	947	7517	11.2	1.1	2.3	24.6	27.6	25.7	23.1	0.32	2.56	40,735	68	537	1.0+6.0+SP
7	2000/09/19	348	1941	15.2	1.1	2.3	15.5	21.9	7.9	15.3	0.31	1.71	19,226	32	176	2.5+1.0+1.5
8	2000/09/26	206	1127	15.5	1.1	1.5	38.9	12.7	37.2	10.5	0.09	0.52	42,751	17	94	2.0+2.5+3.0
9	2000/10/22	278	1083	20.4	1.1	1.2	51.5	15.9	41.8	12.7	0.08	0.3	28,688	9	33	8.0+4.0+3.0
10	2000/10/23	454	1669	21.4	1.2	1.6	43.2	23.7	33.7	15.7	0.08	0.31	99,818	35	128	2.0+3.0+0.5
11	2000/10/23	149	754	16.5	1.2	1.8	41.9	22.9	26.7	15.6	0.04	0.2	50,334	13	68	SP+0.5+4.5
12	2000/10/23	37	176	17.4	1.1	2.0	24.5	30.4	14.1	16.5	0.03	0.14	23,849	5	25	SP+SP+3.0
13	2000/10/23	92	623	12.9	1.2	1.4	48.6	19.6	40.1	15.2	0.06	0.44	22,603	10	69	1.0+3.0+0.5
14	2000/10/23	131	891	12.8	1.1	1.6	29.5	27.4	29.3	18.5	0.09	0.67	13,130	9	59	3.0+3.5+0.5
15	2000/10/24	299	2223	11.9	1.3	1.5	39.9	22.6	29.1	16.2	0.1	0.72	21,292	14	106	1.0+1.5+8.0
16	2001/07/14	779	4808	13.9	1.1	2.5	20.4	17.2	8.3	14.8	0.55	3.4	17,566	56	343	3.0+0.5+2.0
17	2001/08/25	125	544	18.7	2.2	3.2	20.9	20.4	13.1	16.1	0.13	0.58	12,981	14	60	1.5+3.0+0.5
18	2001/08/30	2022	4679	30.2	1.1	2.6	9.4	26.3	8.1	21.1	1.38	3.2	19,314	155	360	2.0+4.0+0.5
19	2001/08/31	56	1505	3.6	1.1	1.9	30.0	26.2	15.3	22.9	0.06	1.7	16,315	8	215	0.5+2.5+1.0
20	2001/09/01	5491	6052	47.6	1.2	2.4	11.9	26.0	9.7	20.3	1.77	1.96	37,421	392	432	1.5+3.5+2.0
21	2001/09/05	947	3554	21.0	1.1	2.4	13.9	18.9	10	15.8	0.86	3.23	17,745	95	355	1.5+2.5+0.5
22	2001/09/06	2037	8799	18.8	1.1	2.4	15.0	23.4	10.6	18.5	1.19	5.13	43,920	226	978	1.0+3.0+1.0
24	2001/09/29	82	325	20.2	1.1	1.6	51.6	57.3	42.5	40.2	0.06	0.23	19,122	7	27	1.5+1.0+3.0
26	2002/06/19	186	948	16.4	1.1	2.3	30.4	22.0	21	15.4	0.26	1.3	16,717	27	135	1.0+2.0+0.5
27	2002/07/08	1498	16434	8.4	1.1	2.6	25.0	24.1	15.3	17.9	0.27	2.98	46,232	75	822	2.0+5.5+4.5
28	2002/07/08	1567	4572	25.5	1.1	2.0	19.4	15.5	9.5	13	0.91	2.64	32,504	174	508	1.0+2.5+0.5
29	2002/08/31	225	2297	8.9	1.0	2.3	11.4	16.7	9.6	14.6	0.21	2.17	18,284	23	230	2.5+2.0+0.5
30	2002/08/09	5099	15888	24.3	1.1	2.8	14.6	23.3	10.4	19.4	0.7	2.18	86,530	300	935	2.0+4.5+2.0
31	2002/08/24	2523	6355	28.4	1.1	2.4	15.3	22.4	10	17.1	1.41	3.56	26,600	194	489	5.0+2.5+0.5
32	2002/08/24	2687	6698	28.6	1.1	2.7	10.7	24.1	8.2	19.7	1.66	4.12	26,348	179	447	5.0+2.0+0.5
33	2002/09/16	204	1387	12.8	1.1	2.1	35.2	32.8	20.2	27.1	0.1	0.61	24,697	15	99	3.5+3.0+1.5
34	2002/09/20	842	8038	9.5	1.1	2.3	27.7	18.8	15	15.3	0.19	1.67	73,679	60	574	3.0+3.0+3.5
35	2002/09/21	4984	4623	51.9	1.2	2.8	9.3	22.5	7.6	18.6	1.18	1.1	43,399	332	308	1.0+4.5+1.5
Mean (standard deviation)				22.3	1.1 (0.5)	2.4 (1.9)	17.0 (26.8)	22.6 (18.6)						89 (155)	309 (370)	

[a] First storms phase duration+growing phase duration+dissipating phase duration.

among the different cases (see Table 1). The maximum value of +CG lightning ratio during a MCS is around 52% (MCS35) and the minimum value hardly surpasses 3.5% (MCS19). The monthly values computed using all CG flashes associated with the MCSs recorded during June, July, August, September or October for the whole period are 28.46, 12.64, 23.12, 26.75 and 19.41, respectively.

These monthly values are higher than those recorded in previous studies for similar months in the area. R01, A01 and RP02 found values lower than 10% during the summer months in the Iberian Peninsula and in the Western Mediterranean region. However, most of these studies considered storms of all types and it is known that MCSs can produce higher percentage of +CG flashes (e.g., Nielsen et al., 1994; Toracinta et al., 1996; MacGorman and Morgenstern, 1998; Parker et al., 2001). In the present work mean values up to 40% are recorded in September. Thus, our results suggest that MCSs can produce higher percentage of +CG flashes than other convective storms.

3.2. Multiplicity

The mean value of the multiplicity (number of strokes per flash) was 1.1 (2.4) for the +CG flashes (−CG flashes). The values of the multiplicity for the +CG flashes show low variability among the different systems, except for MCS17 (see Table 1) which is almost double the overall average. The variability is greater for the −CG flashes, with values ranging from 1.22 to 3.17 (Table 1); the maximum value was also recorded in MCS17.

The mean value of 1.1 obtained for the +CG flashes is identical to that found by R01 for the Iberian Peninsula and by RP02 for the Western Mediterranean region for a 3-year period. On the other hand, the mean value of the −CG flashes averaged for all MCSs is higher than the values obtained by R01 and RP02. In any case, these values (multiplicity of +CG and −CG flashes) are low when compared with other CG lightning detection systems as the Lightning Position and Tracking System (LPATS) (e.g., Montandon et al., 1992; Pinto et al., 1999). Around 91% (49%) of the +CG (−CG) lightning flashes associated with MCSs showed a single-stroke. Tuomi (1996) found values of 88% (63%) for the +CG (−CG) lightning flashes in Finland using the ALDF system. We have observed that as the flash rate increased (when the values are up to 500 flashes per 100 km^2 per 30 min), the percentage of single-stroke −CG flashes is not higher than 60% (Fig. 3). It could be due to instrumentation limitations or to real effects. The ALDF system may be less efficient in discriminating strokes occurring very close in time (Pinto et al., 1999). Also, high flash rates will dissipate the charge faster, perhaps allowing only single-stroke flashes to occur.

3.3. Intensity

The median peak current obtained by using the total number of flashes associated with each MCS of the 33 cases is shown in Fig. 4. The mean value for the +CG (−CG) flashes of all the MCSs is 17.0 kA (22.6 kA). The values of the mean (median) for the +CG flashes of MCSs range between 9.4 and 51.6 kA (7.6–42.5 kA) and for the −CG flashes range between 12.7 and 42.5 kA (10.5–40.2 kA). The monthly averaged values of CG lightning associated with the MCSs are shown in Fig. 5 (June and October are not considered because in June the data are very scarce and all the MCSs detected in October

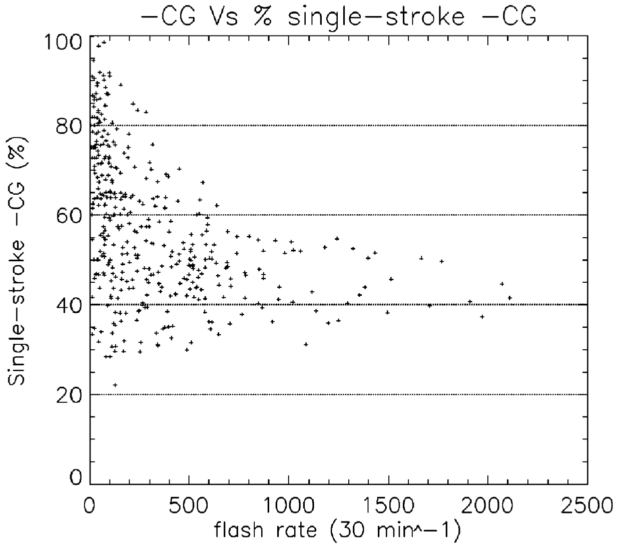

Fig. 3. Distribution of single-stroke −CG flashes as a function of −CG flash rate.

correspond to the same synoptic event and in November and December no MCSs were detected). The highest variability in the values of the averaged peak current is found in September. The monthly mean values are similar to those obtained by others authors over the same area and including different storm types (R01, A01, RP02). This result suggests that the intensity does not depend on storm type.

3.4. CG flash density and rate

The density is calculated as the number of flashes in a certain time period divided by the total area of the MCS. The maximum CG lightning density averaged along the

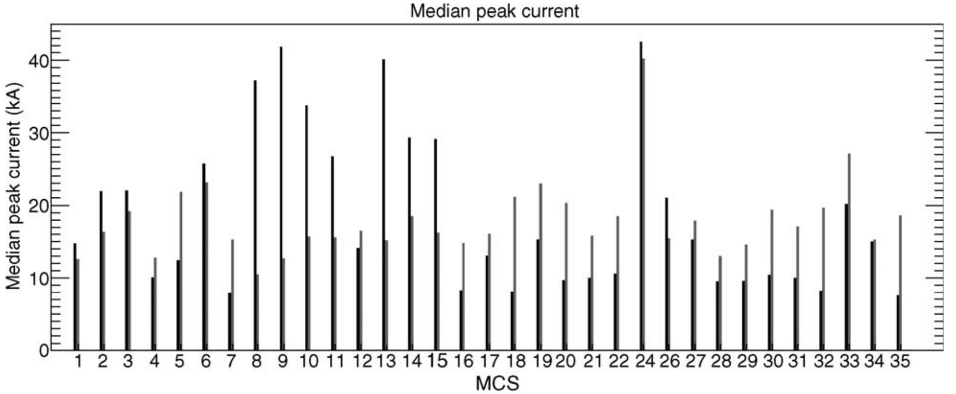

Fig. 4. Absolute values of median peak current value for each MCS. Black and grey bars for +CG flashes and for −CG flashes values, respectively.

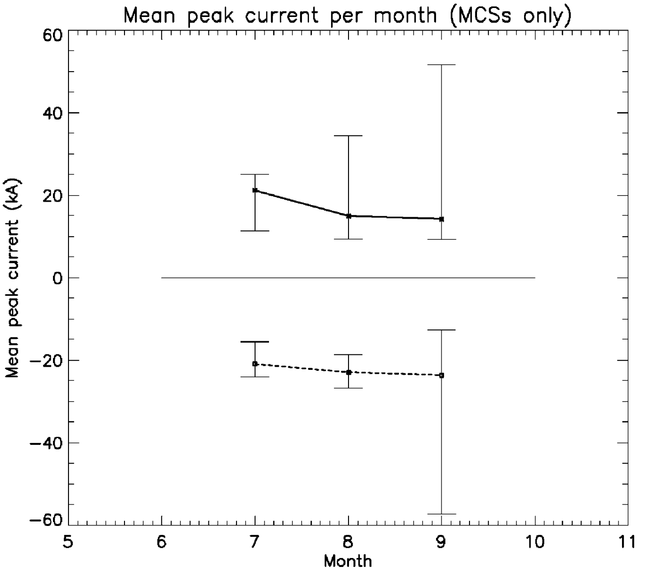

Fig. 5. Monthly average of the peak current of CG lightning associated with the MCSs (a total of 3 MCSs for July, 10 MCSs for August and 11 MCSs for September have been used). Solid line indicates the value for the +CG lightning, dashed line show the value for the −CG lightning whereas the bars indicate the maximum and minimum values of the MCSs observed.

complete life cycle of a MCS corresponds to MCS22. The value was 6.32 flashes (per 100 km^2 per 30 min) and the minimum value was 0.17 flashes (per 100 km^2 per 30 min) for MCS12, with a mean value for the 33 cases of 1.98 flashes (per 100 km^2 per 30 min). The minimum averaged flash rate during the life cycle of a MCS was found for MCS12, with a value of around 1 flash (min^{-1}). The maximum average flash rate for a life cycle of a system was around 41 flashes (min^{-1}). The mean value of flash rate, for all the MCSs, was around 13 flashes (min^{-1}). It has to be remarked that these values are averaged for the duration of the MCS but very intense and very weak periods can alternate affecting to a large extent to the averaged value. Similar values have been found by Parker et al. (2001) and Holle et al. (1994) for MCSs and by Goodman and MacGorman (1986) for MCCs in the United States.

4. Electrical life cycle

The life cycle of a MCS can be established from different points of view, depending on the data used (IR imagery, radar, precipitation, intracloud and/or CG lightning, . . .). In this paper, brightness temperature derived from IR imagery allows an objective and stable classification for the MCSs related with the size of the cloud-top shield of the convective system. The derived life cycle normally comprises a period when the system is growing, a period when the system reaches the maximum extension and a period when the system starts to decrease.

Following the criteria adopted by some authors, the life cycle has been defined using the −52 °C brightness isotherm (Augustine et al., 1989; Riosalido et al., 1998). The duration of each MCS has been divided in four phases: first storms (the period with a −52 °C cloud shield between 1000 and 10000 km^2), growing phase (−52 °C cloud shield from ≥10000 km^2 until the MCS reaches the maximum area), *maximum area* (the period when the MCS holds the maximum area) and *dissipating phase* (since the area starts to decrease until it is lower than 10000 km^2). The *growing,* the *maximum area* and the *dissipating phases* are included in the life cycle used in García-Herrera et al. (2005a). In the present work, the *first storms* phase has been incorporated to include the electrical activity that normally starts before the MCS reaches the initial 10000 km^2 area.

Table 2 shows the mean values of the percentage of the CG flashes occurring during each phase of the MCS for each polarity (i.e. $+CG_{phase\ i}/+CG_{four\ phases}$ and $-CG_{phase\ i}/-CG_{four\ phases}$). The *growing phase* is the period when the maximum percentage of CG flashes occurs both for +CG and −CG and when maximum flash rates are recorded. 75.2% of total CG flashes (82.0% of +CG and 73.4% of −CG flashes) occur during the first two phases (*first storms*+*growing phase*), when MCSs are growing, while 15.9% of total CG flashes are recorded during the *dissipating phase*. It should be kept in mind that the systems suffer mergins and splittings and not all the systems show four phases; additionally, some IR images are not available. This may modify the duration of a phase due to the relative inaccurate detection of the start and end of a phase (see last column of Table 1, the maximum area phase has not been included since it is computed using one IR image, i.e. 0.5 h, for all MCSs). So, the results of this paragraph have to be taken with caution.

Most of the CG lightning flashes associated with MCSs occur before the system reaches the maximum size, while the activity of the +CG flashes is more important during the *first storms* and *growing phases*. Fig. 6 shows the mean density values (flashes per 100 km^2 per 30 min) during each phase. In 23 out of 33 MCSs the *first storms phase* mean density value is the highest. For the −CG lightning flashes, the maximum mean value of the density in a phase occurs during the *first storms phase* in 24 out of 33 cases. This behaviour is obvious if we note that during the *first storms phase* the convection has started but the horizontal expansion at higher levels is not as developed as during the next phases. The CG flash density evolution during the MCS life usually displays a maximum during the *first storms phase*. Both the +CG and the −CG flash densities reach the maximum flash density averaged every 30 min before the maximum cloud-top area of MCSs in around 90% of the convective systems (29 out of 33 MCSs).

In around 70% of the cases (23 out of 33) the maximum flash rate of +CG lightning flashes occurs before the MCS reached its maximum area: for −CG flashes this occurred

Table 2
Mean percentage of +CG and −CG flashes during each phase with respect to total number of +CG and −CG flashes, respectively, during the entire MCS (i.e. $+CG_{phase\ i}/+CG_{four\ phases}$ and $-CG_{phase\ i}/-CG_{four\ phases}$)

MCS	First storms		Growing phase		Maximum area		Decreasing phase	
	% +CG	% −CG	% +CG	% −CG	% +CG	% −CG	% +CG	% −CG
Mean value	21.3	16.1	60.7	57.3	7.2	9.2	10.8	17.4

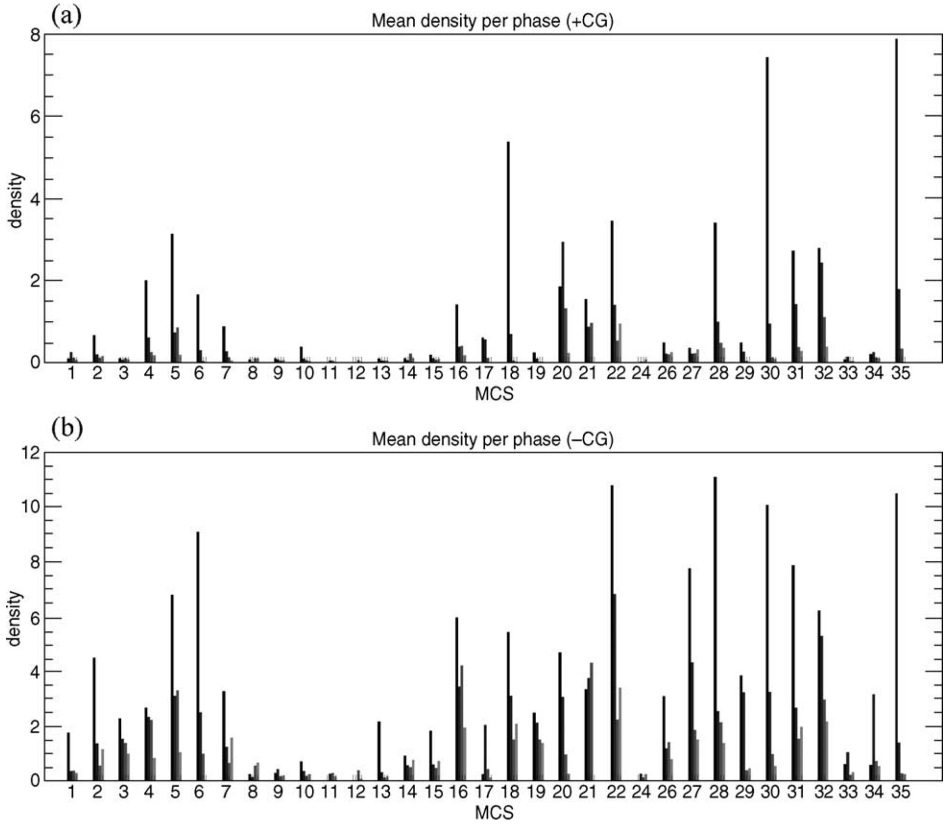

Fig. 6. Mean density values ((number of flashes) per 100 km^2 per 30 min) of the (a) +CG lightning flashes and the (b) −CG lightning flashes during each phase of the MCS life cycles (black bars indicate the mean value during the *first storm* phase with the dark grey color for the *growing phase*, the mid grey color for the *maximum area phase* and light grey color for the *dissipating phase*).

in 20 cases. An example is shown in Fig. 7 that corresponds to MCS9. It can be seen that the maximum occurrence of +CG flashes occurs before that for the −CG flashes and before the maximum area. In average, the percentage of +CG flashes is 27.7 during the *first storm phase*; decreasing steadily along the rest phases, with values of 23.5, 18.3 and 15.2, respectively.

The evolution of the percentage of single-stroke +CG and −CG flashes during the different phases of a MCS has been examined (Fig. 8). No trend can be identified for +CG flashes, whereas higher values have been found for −CG flashes as the system evolves.

5. Discussion

Our results show that MCSs occurring in the Western Mediterranean region exhibit higher average values of +CG lightning flashes percentage than other types of storms.

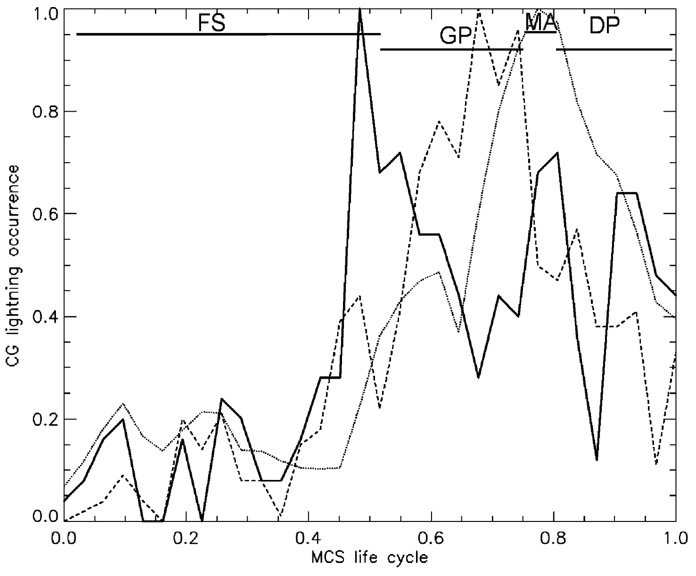

Fig. 7. Evolution of the +CG flash rate (solid line), −CG flash rate (dashed line) and of the −52 °C cloud shield area (dotted line) for the MCS09. The values of the CG flash rate (number of flashes in a 30-min period) and the values of the area are normalized. The duration of the life cycle (First storms (FS)+growing phase (GP)+maximum area (MA)+dissipating phase(DP)) is also normalized. The flash rates and area were normalized by their maximum value during the storm, i.e. values of 25 for the +CG, 100 for the −CG and 28,688 km^2 for the area.

Rutledge and MacGorman (1988) suggest that the source of +CG flashes in MCSs is related with the transport of positive charge contained in the ice particles. Additional evidences (Engholm et al., 1990; Rutledge et al., 1990; Nielsen et al., 1994) suggest that the charge generation in the stratiform precipitation zone is probably more important than the advection of positive charge from the convective line. Recently, Schuur and Rutledge (2000) used a bidimensional model of MCS to conclude that the charge advection from the convective line is more important in the upper charge layers in the stratiform rain region, whereas the charge generation could be more important in the lower.

The average percentage of +CG strikes is higher during the *first storm*s *phase*, decreasing in the subsequent phases. An example of this behaviour can be seen in Fig. 9. Morgenstern (1991) found two characteristic modes of evolution of MCSs, the *convective mode*, with a majority of CG (+CG and −CG) flashes concentrated in the same area and high percentage of +CG flashes during the early stages of the storm, and the *stratiform/dissipating mode*, with most of +CG flashes scattered in areas far from the main high density areas (majority of −CG flashes) of the MCS and low percentage of +CG flashes. In our study a total of 7 MCSs exhibit the *convective mode*, 3 cases show the *stratiform/dissipating mode*, whereas the rest display a mixed behaviour.

The CG flash evolution over the entire lifetime shows that, generally, +CG and −CG flash counts increase rapidly from the initiation of the *first storms phase* until the flash rate reaches the maximum value during the *growing phase*, i.e. before the area reaches its

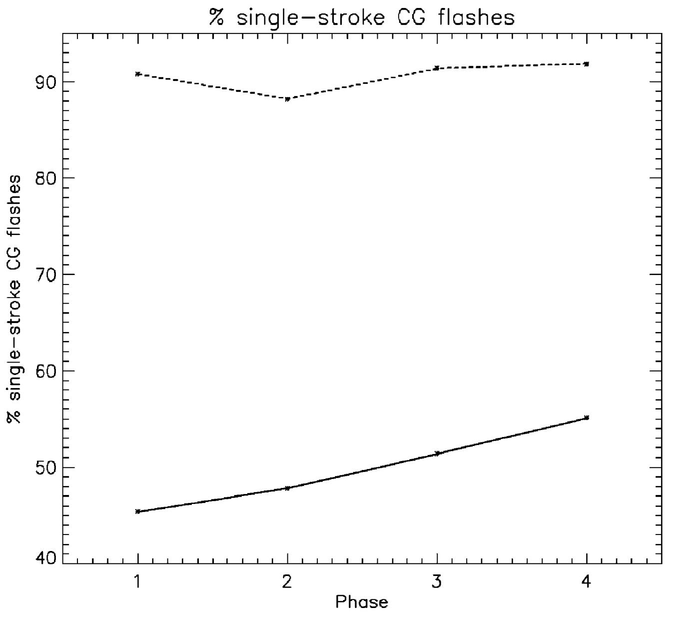

Fig. 8. Percentage of single-stroke −CG flashes (solid line) and +CG flashes (dotted line). Numbers in the x-axis indicate the corresponding phase with 1, 2, 3 and 4 assigned to *first storms phase, growing phase, maximum area phase* and *dissipating phase*, respectively.

maximum extent. Usually, the counts of CG flashes decrease rapidly from the maximum flash rate until the final dissipation of the MCS. Generally, the maximum +CG flash rate occurs before the −CG flash rate and during the first two phases the +CG flash percentage is higher than during the rest. High +CG flash rates in initial stages of storms with hail production have been reported in several studies (Stolzenburg, 1994; Nielsen et al., 1994). Goodman and MacGorman (1986) in their analysis of 10 MCCs in the United States found a similar behaviour of CG flash temporal evolution, although they did not distinguish between +CG and −CG flashes. The evolution of ground flash rates is similar in MCSs and MCCs (Morgenstern, 1991). Our results are consistent with these previous studies which associate this −CG flashes pattern with deep convection in MCSs.

As Morgenstern (1991), we have observed that −CG flash rates tend to show the maximum values when the cloud tops of MCSs attained their coldest temperature. This can be seen in Fig. 10, where 27 out of 33 cases show the maximum flash rate in an interval ±1 h around the time of coldest cloud-top temperature. For the +CG flashes the maximum flash rate usually occurs before the maximum flash rate of negative ground flashes (e.g., Fig. 7).

São Sabbas and Sentman (2003) found that compact regions of very cold cloud tops develop as the storm grows and the lightning discharges, −CG more than +CG flashes, have the tendency to concentrate on those regions. Similar results have been found in the present study (e.g., Fig. 2). The position of the CG in the MCS cloud-top temperature structure has been analyzed in a ±5-min interval centered in the time of the IR imagery.

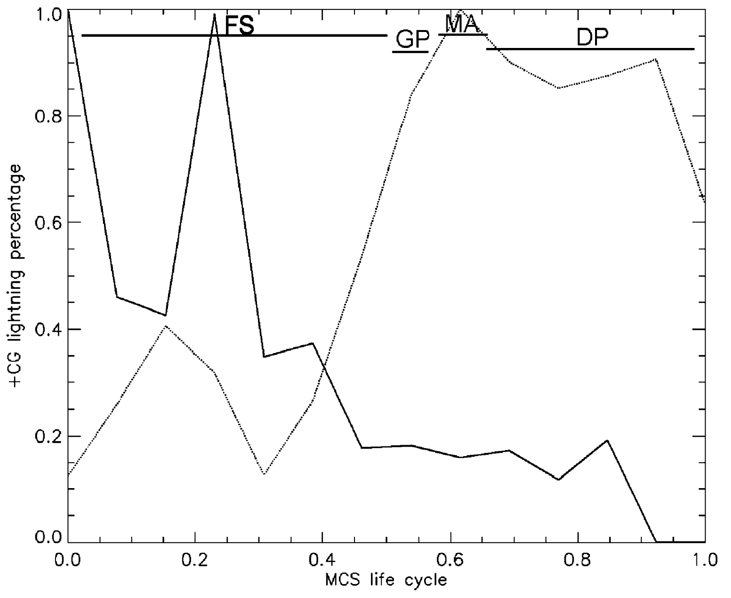

Fig. 9. Evolution of the percentage of +CG flashes (solid line) and the −52 °C cloud shield (dotted line) during the life cycle of MCS16 (normalized values). The duration of the life cycle (First storms (FS)+growing phase (GP)+maximum area (MA)+dissipating phase(DP)) is also normalized. The percentage of +CG flashes and area were normalized by their maximum value during the storm, i.e. values of 56.5 for the percentage of +CG flashes and 17,566 km^2 for the area.

An example can be seen in Fig. 11. Around 63% of CG flashes were in areas colder than −56 °C (this area can be less than 50% of the −52 °C area; e.g., see Figs. 2 and 11) whereas the rest were in areas of temperature between −52 °C and −56 °C. These results show that the use of IR imagery and lightning data to detect and follow convective areas in cases when radar data are not available is useful.

MCSs with mean density during the entire life cycle lower than 1.00 flashes (30 min^{-1} 100 km^{-2}) (see Table 1) show median peak current values higher than the rest. When the +CG flash density is high then the median (and the mean) peak current is low. Fig. 12 shows the curve adjusted to the mean values of the +CG flash peak current as a function of the +CG flash density averaged during the life cycle. The correlation coefficient obtained is 0.84 (p<0.01). MacGorman and Morgenstern (1998) found similar results when analysing the distributions of the median peak current as a function of the number of ground flashes. They divided their results into three categories and suggested that the median peak current depends on the flash rates of +CG flashes. Petersen and Rutledge (1992) suggested that the large horizontal area of the stratiform region stores more charge than the convective regions; and thus they can produce larger peak currents. MacGorman and Morgenstern (1998) observed a tendency for the median peak current of +CG flashes to increase with increasing cloud area for MCSs that produced +CG flashes in the stratiform region, though with exceptions. However, MacGorman and Morgenstern (1998) found that this hypothesis does not

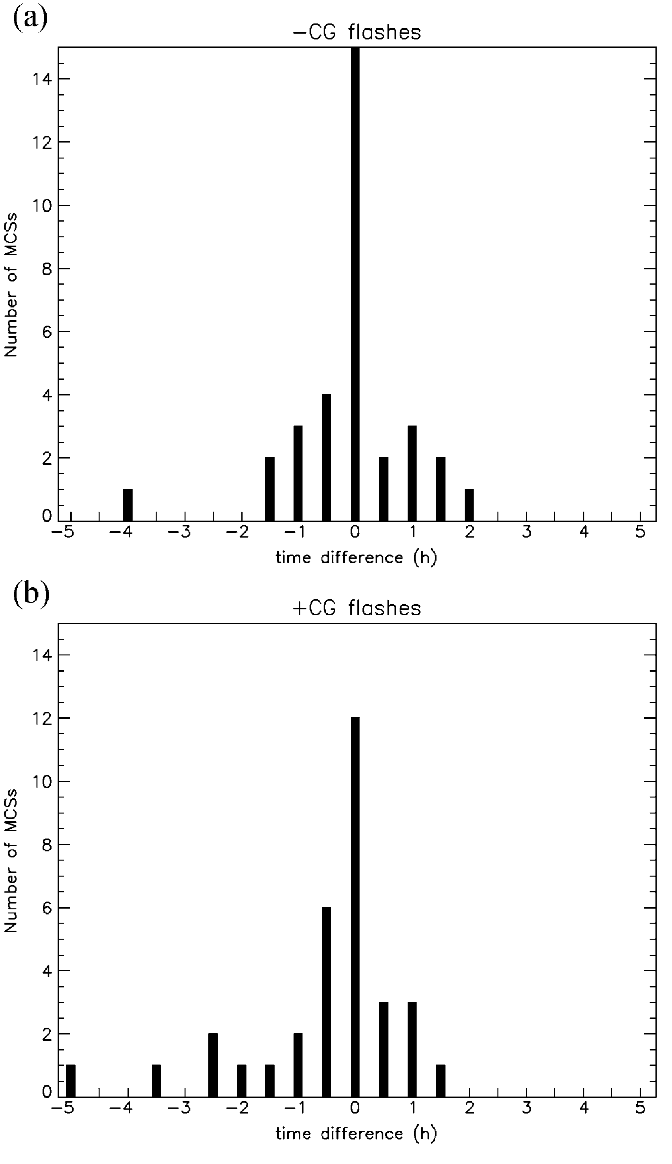

Fig. 10. Time difference between the maximum flash rate and the minimum cloud-top brightness temperature for (a) −CG and (b) +CG lightning strikes. The moment of the coldest cloud-top temperature is set to 0 in the *x* axis.

explain why some MCSs that produced +CG flashes mainly in the convective region also produced large median peak currents, though their area was among the smallest in their dataset. We have not found any relationship between the area of the MCSs and the mean or median peak current of the +CG flashes. On the other hand, the median peak current is independent of the flash density for the −CG flashes, in agreement with MacGorman and Morgenstern (1998). Our analysis shows that when the values of the

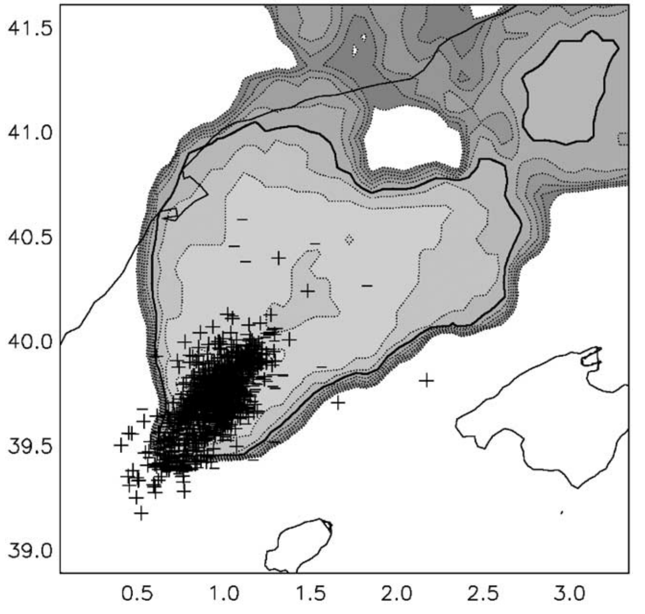

Fig. 11. MCS35 at 0830 UTC on 21 September 2002. The shaded contours indicate 4 °C brightness temperature intervals starting in −32 °C (darker). The wide solid line indicates the −52 °C cloud shield during the 0825–0835 UTC interval. '+' and '−' indicate the position of the positive and negative CG flashes, respectively. The thin solid line indicates the coastlines.

−CG flash density are high, the median peak current values range between −10 kA and −30 kA.

Summing up our results:

– MCSs occurred in the Western Mediterranean show a high percentage of +CG flashes in relation with studies made in the same area for some years including all type of storms.
– The +CG flash percentage during the first phase of the storm is higher (in mean values) than in the rest of the following phases (decreasing the percentage in the next phases).
– A third part of the systems can be classified as convective or stratiform/dissipating, while the rest have a mixed behaviour, regarding the modes of evolution described in Morgenstern (1991).
– Most of the CG lightning flashes associated with a MCS occur before the system reaches the maximum size, i.e. the maximum cloud shield within the −52 °C brightness isotherm, and the peak flash rate of +CG flashes usually occurs before than that of the −CG flashes during the lifetime of a MCS.
– Most of CG flashes tend to be located in regions of very cold cloud-top temperatures and the maximum flash rate coincides with the minimum cloud-top temperature.

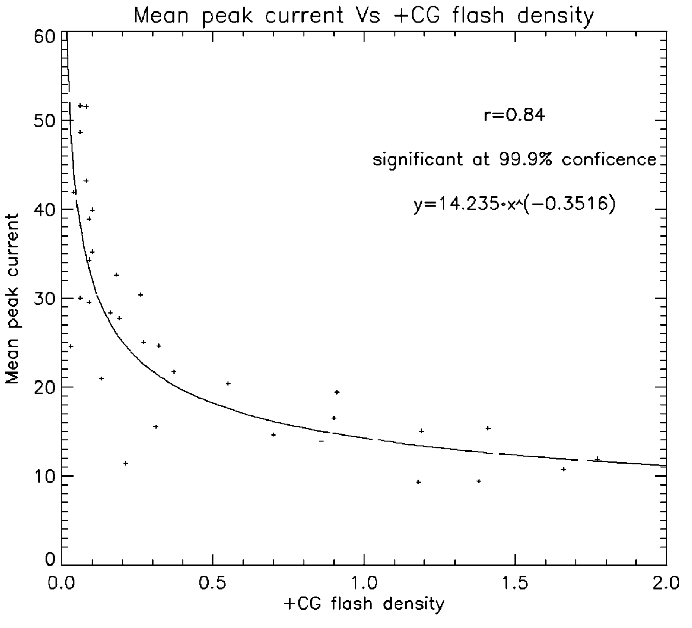

Fig. 12. Distribution of mean peak current of +CG flashes as a function of +CG flash density averaged during the life cycle for each MCS. The solid line is the fitted regression curve.

– The mean and median peak current for +CG flashes are related with the CG flash density and rate, whereas the mean or median peak current for −CG flashes were independent of CG flash rate or density.

Acknowledgments

The authors wish to thank the INM for providing the CG lightning data used in the development of the paper. Our thanks also to the two anonymous referees of this paper for their interesting suggestions and comments.

References

Areitio, J., Ezcurra, A., Herrero, I., 2001. Cloud-to-ground lightning characteristics in the Spanish Basque Country area during the period 1992–1996. J. Atmos. Sol.-Terr. Phys. 63, 1005–1015.

Augustine, J.A., Tollerud, E.I., Jamison, B.D. 1989. Distributions and other general characteristics of mesoscale convective systems during 1986 as determined from GOES infrared imagery. Pp. 437-442 in preprint volume of the 12th Conference on weather analysis and forecasting, 2–6 October 1989, Monterey, CA, USA.

Carretero, O., Riosalido, R., 1996. Características satélite de los sistemas convectivos de mesoescala en las proximidades de la Península Ibérica en el período 1989–1993. Proceedings of the IV Simposio Nacional de Predicción, Memorial “Alfonso Ascaso”, 15–19 April 1996, Madrid, Spain.

Carvalho, L.M.V., Jones, C., 2001. A satellite method to identify structural properties of Mesoscale Convective Systems Based on the Maximum Spatial Correlation Tracking Technique (MASCOTTE). J. Appl. Meteorol. 40, 1683–1701.

Cummins, K.L., Krider, E.P., Malone, M.D., 1998. The U.S. national lightning detection network and applications of cloud-to-ground lightning data by electric power utilities. IEEE Trans. Electromagn. Compat. 40, 465 – 480.

Engholm, C.D., Williams, E.R., Dole, R.M., 1990. Meteorological and electrical conditions associated with positive cloud-to-ground lightning. Mon. Weather Rev. 118, 470 – 487.

Finke, U., Hauf, T., 1996. The characteristics of lightning occurrence in Southern Germany. Contrib. Atmos. Phys. 69, 361 – 374.

García-Herrera, R., Barriopedro, D., Hernández, E., Paredes, D., Correoso, J.F., Prieto, L., 2005a. The 2001 Mesoscale Convective Systems over Iberia and the Balearic Islands. Meteorol. Atmos. Phys. DOI:10.1007/s00703-005-0114-2.

García-Herrera, R., Hernández, E., Paredes, D., Barriopedro, D., Correoso, J.F., Prieto, L., 2005b. A MASCOTTE based characterization of MCSs over Spain, 2000–2002. Atmos. Res. 73, 261 – 282.

Goodman, S.J., MacGorman, D.R., 1986. Cloud-to-Ground lightning activities in Mesoscale Convective Complexes. Mon. Weather Rev. 114, 2320 – 2328.

Hernández, E., Cana, L., Díaz, J., García-Herrera, R., Gimeno, L., 1996. Mesoscale convective complexes over the Western Mediterranean area during 1990–1994. Meteorol. Atmos. Phys. 68, 1 – 12.

Holle, R.L., Watson, A.I., López, R.E., MacGorman, D.R., 1994. The life cycle of lightning and severe weather in a 3–4 June 1985 PRE-STORM mesoscale convective system. Mon. Weather Rev. 122, 1798 – 1808.

Homar, V., Romero, R., Ramis, C., Alonso, S., 2002. Numerical study of the October 2000 torrential precipitation event over eastern Spain: analysis of the synoptic-scale stationarity. Ann. Geophys. 20, 2047 – 2066.

Krider, E.P., Noggle, A.E., Uman, M.A., 1976. A gate, wideband magnetic direction finder for lightning return strokes. J. Appl. Meteorol. 15, 301 – 306.

Lopez, R.E., Holle, R.L., 1986. Diurnal and spatial variability of lightning activity in northeastern Colorado and central Florida during the summer. Mon. Weather Rev. 114, 1288 – 1312.

MacGorman, R.D., Morgenstern, C.D., 1998. Some Characteristics of cloud-to-ground lightning in mesoscale convective systems. J. Geophys. Res. 103, 14011 – 14023.

Machado, L.A.T., Rossow, W.B., Guedes, R.L., Walker, A.W., 1998. Life cycle variations of mesoscale convective systems over the Americas. Mon. Weather Rev. 126, 1630 – 1654.

Martín León, F., 1995. Actividad tormentosa en la Península y áreas limítrofes durante el verano de 1994. TECH. NOTE 23, INM, Madrid, Spain. 27 pp.

Molinie, G., Soula, S., Chauzy, S., 1999. Cloud-to-ground lightning activity and radar observations of storms in the Pyrenees range area. Q. J. R. Meteor. Soc. 125, 3103 – 3122.

Montandon, E., Ahnebrik, J., Brent, R.B., 1992. Analysis of lightning density and recorded waveforms by the Swiss lightning position and tracking system. Paper Presented at 21st International Conference on Lightning Protection. VDE, Berlin, Germany.

Morel, C., Senesi, S., 2002. Climatology of European MCSs. II. Q. J. R. Meteor. Soc. 128, 1973 – 1995.

Morgenstern, C.D., 1991. Cloud-to-ground lightning characteristics in mesoscale convective systems. April–September 1986, MS Thesis, University of Oklahoma, 109 pp.

Nielsen, K.E., Maddox, R.A., Vasiloff, S.V., 1994. The evolution of cloud-to-ground lightning within a portion of the 10–11 June 1985 squall line. Mon. Weather Rev. 122, 1809 – 1817.

Orville, R.E., 1994. Cloud-to-ground lightning flash characteristics in the contiguous United States: 1989–1991. J. Geophys. Res. 99, 10833 – 10841.

Orville, R.E., Henderson, R.W., Bosart, L.F., 1983. An east coast lightning detection network. Bull. Am. Meteorol. Soc. 64, 1029 – 1037.

Parker, M.D., Rutledge, S.A., Johnson, R.H., 2001. Cloud-to-Ground lightning in linear Mesoscale Convective systems. Mon. Weather Rev. 129, 1232 – 1242.

Petersen, W.A., Rutledge, S.A., 1992. Some characteristics of cloud-to-ground lightning observations in tropical northern Australia. J. Geophys. Res. 97, 11553 – 11560.

Pinto, I.R.C.A., Pinto Jr., O., Rocha, R.M.L., Diniz, J.H., Carvalho, A.M., Cazeta Filho, A., 1999. Cloud-to-ground lightning in Southeastern Brazil in 1993. 2: time variations and flash characteristics. J. Geophys. Res. 104, 31381 – 31387.

Riosalido, R., Elizaga, F., Carretero, O., Martín F., 1998. Satellite climatology of Mesoscale convective systems in the surroundings of the Iberian Peninsula: application to torrential rainfall detection (in Spanish). Tech. note (STAP), 29, INM.

Rivas, L., De Pablo, F., 2002. Maritime cloud-to-ground lightning: the Western Mediterranean sea. J. Geophys. Res. 107.

Rivas, L., De Pablo, F., García, E., 2001. Cloud-to-ground lightning activity in the Iberian Peninsula: 1992–1994. J. Geophys. Res. 106, 11891–11901.

Romero, R., Doswell III, C.A., Ramis, C., 2000. Mesoscale numerical study of two cases of long-lived quasi-stationary convective systems over Eastern Spain. Mon. Weather Rev. 128, 3731–3751.

Romero, R., Doswell III, C.A., Riosalido, R., 2001. Observations and fine-grid simulations of a convective outbreak in Northeastern Spain: importance of diurnal forcing and convective cold pools. Mon. Weather Rev. 129, 2157–2182.

Rutledge, S.A., MacGorman, D.R., 1988. Cloud-to-ground lightning activity in the 10–11 June 1985 mesoscale convective system observed during Oklahoma–Kansas PRE-STORM project. Mon. Weather Rev. 116, 1393–1408.

Rutledge, S.A., Lu, C., MacGorman, D.R., 1990. Positive cloud-to-ground lightning in mesoscale convective systems. J. Atmos. Sci. 47, 2085–2100.

São Sabbas, F.T., Sentman, D.D., 2003. Dynamical relationship of infrared cloudtop temperatures with occurrence rates of cloud-to-ground lightning and sprites. Geophys. Res. Lett. 30, 1236.

Schuur, T.J., Rutledge, S.A., 2000. Electrification of stratiform regions in mesoscale convective systems: Part II. two-dimensional numerical model simulations of a symmetric MCS. J. Atmos. Sci. 57, 1986–2006.

Soula, S., Sauvageot, H., Molinié, G., Mesnard, F., Chauzy, S., 1998. The CG lightning activity of a storm causing a flash-flood. Geophys. Res. Lett. 25 (8), 1181–1184. doi:10.1029/98GL00517.

Stolzenburg, M., 1994. Observations of high ground flash densities of positive lightning in summertime thunderstorms. Mon. Weather Rev. 122, 1740–1750.

Toracinta, E.R., Mohr, K.I., Zipser, E.J., Orville, R.E., 1996. A comparison of WSR-88D reflectivities, SSM/I brightness temperatures, and lightning for mesoscale convective systems in Texas: Part I. radar reflectivity and lightning. J. Appl. Meteorol. 35, 902–918.

Tuduri, E., Ramis, C., 1997. The environments of significant convective events in the Western Mediterranean. Weather Forecast. 12, 294–306.

Tuomi, T.J., 1996. Lightning observation in Finland. Fin Meteorol Inst, Helsinki, Finland. 33 pp.